The Hydroxyl Radical Reaction Rate Constant and Products of 3,5-Dimethyl-1-hexyn-3-ol

J. R. WELLS

Exposure Assessment Branch, Health Effects Laboratory Division, National Institute for Occupational Safety and Health, 1095 Willowdale Road, Morgantown, WV 26505

Received 9 January 2004; accepted 14 May 2004

DOI 10.1002/kin.20027
Published online in Wiley InterScience (www.interscience.wiley.com).

ABSTRACT: A bimolecular rate constant, k_{DHO}, of $(29 \pm 9) \times 10^{-12}$ cm^3 molecule^{-1} s^{-1} was measured using the relative rate technique for the reaction of the hydroxyl radical (OH) with 3,5-dimethyl-1-hexyn-3-ol (DHO, HC≡CC(OH)(CH_3)CH$_2$CH$(CH_3)_2$) at (297 ± 3) K and 1 atm total pressure. To more clearly define DHO's indoor environment degradation mechanism, the products of the DHO + OH reaction were also investigated. The positively identified DHO/OH reaction products were acetone ($(CH_3)_2$C=O), 3-butyne-2-one (3B2O, HC≡CC(=O)(CH_3)), 2-methyl-propanal (2MP, H(O=)CCH$(CH_3)_2$), 4-methyl-2-pentanone (MIBK, CH_3C(=O)CH$_2$CH$(CH_3)_2$), ethanedial (GLY, HC(=O)C(=O)H), 2-oxopropanal (MGLY, CH_3C(=O)C(=O)H), and 2,3-butanedione (23BD, CH_3C(=O)C(=O)CH_3). The yields of 3B2O and MIBK from the DHO/OH reaction were (8.4 ± 0.3) and (26 ± 2)%, respectively. The use of derivatizing agents *O*-(2,3,4,5,6-pentalfluorobenzyl)hydroxylamine (PFBHA) and *N*,*O*-bis(trimethylsilyl)trifluoroacetamide (BSTFA) clearly indicated that several other reaction products were formed. The elucidation of these other reaction products was facilitated by mass spectrometry of the derivatized reaction products coupled with plausible DHO/OH reaction mechanisms based on previously published volatile organic compound/OH gas-phase reaction mechanisms. © 2004 Wiley Periodicals, Inc.* Int J Chem Kinet 36: 534–544, 2004

INTRODUCTION

It is estimated that over 30 million of the total 89 million workers in indoor environments are affected by the work environment in the form of eye, nose, and throat irritations, headache, and fatigue. These health complaints have an estimated impact on worker productivity of tens of billions of dollars annually [1,2]. Unfortunately, there is currently no direct correlation between these complaints and a specific pollutant. In fact, exposures to multiple pollutants in the indoor environment may be responsible [3–9].

A recent review of indoor environment chemistry by Weschler highlights several research areas important to the field [10]. Significant observations from this review paper are that there are still several fundamental unanswered questions regarding the gas-phase chemistry

Correspondence to: J. R. Wells; e-mail: rwells@cdc.gov.

of indoor environments, and the indoor environment is chemically more complex than was previously thought. Experimental evidence has implicated that several initiator species such as ozone (O_3), hydroxyl radical (OH), and nitrate radical (NO_3) are likely to be present indoors and the VOC concentrations indoors are higher by a factor of 10 or more than typically found in outdoor environments [10,11].

Oxygenated organic compounds, such as ethers, alcohols, and esters, are becoming more prevalent in the environment as they are substituted for other chemicals in consumer products. While several hydroxyl radical (OH) + oxygenated organic bimolecular rate constants are well known, details pertaining to the OH + oxygenated organic compound reaction mechanisms are limited [12,13]. A few recent studies of the products from OH + oxygenated organic reactions have illustrated the complexity of their gas-phase reaction mechanisms [14–20]. These investigations are needed to support hydroxyl radical reaction mechanism patterns based on chemical structure reactivity relationships [21].

As a side benefit, understanding the compounds' gas-phase mechanisms in detail can provide a basis for chemical selection based on structure. There is the possibility of synthesizing new compounds that incorporate environmentally and technically beneficial molecular structures. The information gained from the type of research presented here can lead to more beneficial use of these and similar compounds in the future.

3,5-Dimethyl-1-hexyn-3-ol (DHO, $HC{\equiv}CC(OH)(CH_3)CH_2CH(CH_3)_2$) is a volatile oxygenated organic compound formed in the indoor environment as a result of cleavage of 2,4,7,9-tetramethyl-5-dicyne-4,7-ol (T4MDD, $(CH_3)_2HCH_2C(CH_3)(HO)(CC{\equiv}CC(OH)(CH_3)CH_2CH(CH_3)_2$), a wetting and defoaming agent in many water-based lacquer systems [22,23]. DHO was observed in experimental chambers as an emission from finished wood furniture as well as from pure T4MDD [23]. Most investigations of alkyne/OH reactions have been on smaller unsubstituted alkynes such as acetylene, [12,13,24–28], propyne [12,25], and 1-butyne [12,25]; however, DHO's structure has the unique combination of a carbon–carbon triple bond with a neighboring alcohol group.

In the work presented here, the rate constant of the OH radical with DHO was measured by the relative rate method [29]. The products of the OH + DHO reaction are also reported and used to derive DHO's indoor environment reaction mechanism. Neither the OH rate constant nor the reaction mechanism for DHO has been reported previously.

EXPERIMENTAL METHODS

Apparatus and Materials

Experiments to measure the gas-phase rate constant of the OH + 3,5-dimethyl-1-hexyn-3-ol (DHO, $HC{\equiv}CC(OH)(CH_3)CH_2CH(CH_3)_2$) reaction were conducted with a previously described apparatus [18,29–31]. A brief description is provided here. Reactants were introduced and samples were withdrawn through a 6.4-mm Swagelok fitting attached to a 60–100 L Teflon® film chamber. Dry compressed air was added as a diluent to the reaction chambers and measured with a 0–100 L min^{-1} mass flow controller (MKS, Andover, MA). The filler system was equipped with a syringe injection port facilitating the introduction of both liquid and gaseous reactants into the chambers by a flowing airstream. All reactant mixtures and calibration standards were generated by this system. Irradiations were carried out in a light-tight chamber using 5-mL FEP Teflon® film bags (60–100 L), which were surrounded by the following mix of lamps: six Philips TL40W/03, one GE F40BL, two QPANEL UV351, and seven QPANEL UV340. This lamp mixture approximates solar radiation from 300 to 450 nm.

All reaction kinetic samples were quantitatively monitored using an Agilent (Palo Alto, CA) 6890 gas chromatograph with a 5973 mass selective detector (GC/MS) and Agilent series Chem Station software. Gas samples were cryogenically collected employing an Entech (Simi Valley, CA) 7100 sampling system utilizing the following trap and temperature parameters: 50 mL of chamber contents were collected onto Trap 1 (packed with Tenax TA) at −150°C. After sample collection, Trap 1 was heated to 40°C and the sample transferred under a flow of ultra high purity helium (UHP He) onto Trap 2 (packed with Tenax TA) cooled to −30°C. Trap 2 was then heated to 180°C and the sample transferred under a UHP He flow onto Trap 3, a silanized 0.53-mm i.d. tube cooled to −160°C, which was subsequently heated to 220°C to inject the sample onto the GC column [Restek (Bellefonte, PA) FAMEWAX (0.25-mm i.d., 30 m long, 0.25 μm film thickness)]. These series of cryogenic trap manipulations reduced the background water level, ensured consistency of replicate samples, and improved the chromatograph peak shapes. The GC temperature program used had an initial temperature of 45°C held for 8 min after sample injection, which was increased 10°C/min to 220°C and held for 4 min. The Agilent 5973 mass selective detector was tuned using perfluorotributylamine (FC-43). Full scan electron impact ionization spectra were collected

from m/z 35 to 220. Preliminary compound identifications from the Agilent 6890/5973 GC/MS data sets were made by searching the NIST 98 Mass Spectral Library.

Reaction product identification experiments were performed utilizing two methods: direct gas-phase sampling and Agilent 6890/5973 GC/MS analysis of the reaction chamber contents as described above or collection and derivatization of gas-phase aldehydes and ketones using *O*-(2,3,4,5,6-pentafluorobenzyl)-hydroxylamine (PFBHA) only, and PFBHA with additional derivatization of alcohols or carboxylic acids using *N*, *O*-bis(trimethylsilyl)trifluoroacetamide (BSTFA) followed by analysis using a Varian (Palo Alto, CA) 3800/Saturn 2000 GC/MS system [32]. The combination of PFBHA/BSTFA derivatizations was used previously to identify the reaction products and propose reaction mechanisms for the ozonolysis of α-pinene and Δ^3-carene [32,33]. Experimental methods for reaction product identification were similar to methods used for kinetic experiments, except that the reference compound was excluded from the reaction mixture.

The derivatized aldehydes, ketones, and alcohols were analyzed with a Varian 3800 gas chromatograph and a Varian Saturn 2000 ion trap mass spectrometer operated in the EI mode. Compound separation was achieved by a J&W Scientific DB-5MS (0.32 mm i.d., 30 m long, 1 μm film thickness) column and the following GC oven parameters: 60°C for 1 min, then 10°C/min to 280°C and held for 10 min. Samples were injected in the splitless mode, and the GC injector was returned to split mode 1 min after sample injection, with the following injector temperature parameters: 60°C for 1 min, then 180°C/min to 250°C and held to the end of the chromatographic run [32]. The Saturn 2000 ion trap mass spectrometer was tuned using perfluorotributylamine (FC-43). Full scan electron impact ionization spectra were collected from m/z 40 to 650.

OH radicals, one of the primary oxidizing radicals in the indoor environment [11,34–36], were generated from the photolysis of methyl nitrite (CH_3ONO) in the presence of nitric oxide (NO) in air [29].

$$CH_3ONO + h\nu \rightarrow CH_3O + NO \quad (1)$$

$$CH_3O + O_2 \rightarrow CH_2O + HO_2 \quad (2)$$

$$H_2O + NO \rightarrow OH + NO_2 \quad (3)$$

CH_3ONO was prepared in gram quantities using the method of Taylor et al. [37] and stored in a lecture bottle at room temperature. The CH_3ONO purity (>95%) was verified by GC/MS.

All compounds were used as received and had the following purities: from Sigma-Aldrich: hexane (99%), decane (99%), 3-butyne-2-one (95%), 3,5-dimethyl-1-hexyn-3-ol (99%), 4-methyl-2-pentanone (99.5%), acetonitrile (99.93%), *N*,*O*-bis-(trimethyl silyl) trifluoroacetamide (BSTFA) (>99%), *O*-(2,3,4,5,6-pentafluorobenzyl)hydroxylamine hydrochloride (PFBHA) (>98%); from Ultrascientific: pentanal (98%), 2-methyl propanal (98%); from Fisher Scientific: methanol (99%); from Acros: 2,3-butanedione (99%); from Spectrum Analytical: methylene chloride (99.5%). Water was distilled, deionized to a resistivity of 18 M Ω cm, and filtered using a Milli-Q® filter system. Nitric oxide (>99% pure) was obtained as a 4942-ppm mixture in nitrogen from Butler Gases (Morrisville, PA). Helium (UHP grade), the carrier gas, was supplied by Amerigas (Sabraton, WV) and used as received. Experiments were carried out at (297 ± 3) K and 1-atm pressure.

Experimental Procedures

The experimental procedures for determining the DHO + OH reaction kinetics were similar to those described previously [19,20].

$$DHO + OH \xrightarrow{k_{DHO}} Products \quad (4)$$

$$Reference + OH \xrightarrow{k_R} Products \quad (5)$$

The rate equations for reactions (4) and (5) are combined and integrated, resulting in the following equation:

$$\ln\left(\frac{[DHO]_0}{[DHO]_t}\right) = \frac{k_{DHO}}{k_R} \ln\left(\frac{[R]_0}{[R]_t}\right) \quad (6)$$

If reaction with OH is the only removal mechanism for DHO and reference, a plot of $\ln([DHO]_0/[DHO]_t)$ versus $\ln([R]_0/[R]_t)$ yields a straight line with an intercept of zero. Multiplying the slope of this linear plot by k_R yields k_{DHO} (Fig. 1). The OH rate constant experiments for DHO employed the use of two reference compounds, decane and pentanal. The use of two different reference compounds with different OH rate constants more definitively assured the accuracy of the DHO/OH rate constant and demonstrated that other reactions were not removing DHO.

For the DHO/OH kinetic experiments, the typical concentrations of the pertinent species in the 60–100 L Teflon® chamber were 0.3–1-ppm DHO, 0.7–8-ppm reference, 10–100-ppm CH_3ONO, and 0.6-ppm NO in air. These mixtures were allowed to mix for 30–60 min before initial species concentration

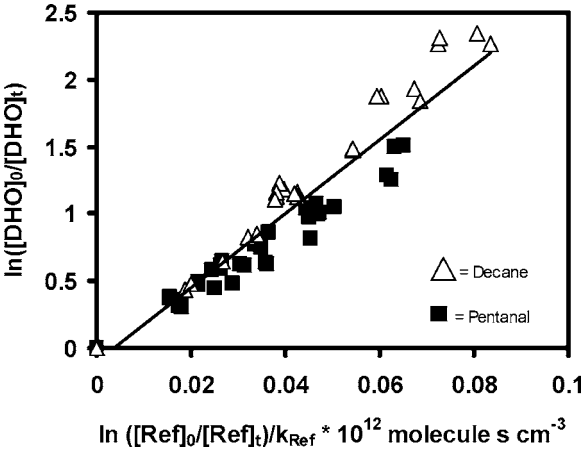

Figure 1 3,5-Dimethyl-1-hexyn-3-ol relative rate plot with decane (△) and pentanal (■) as reference compounds. The OH + DHO rate constant, k_{DHO}, measured is (28.8 ± 1.2) × 10^{-12} cm^3 $molecule^{-1}$ s^{-1}.

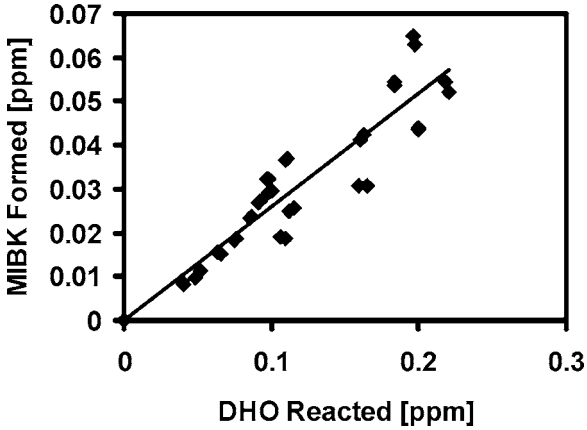

Figure 2 Plot of 4-methyl-2-pentanone (MIBK) formed, corrected for MIBK/OH reaction, versus DHO reacted. The slope of the linear least squares analysis with 95% confidence interval is 0.26 ± 0.2.

($[X]_0$) samples were collected. Typically, four photolysis intervals of 2 to 10 s each were used on the reaction mixture for a combined total photolysis time of approximately 8–40 s. The total ion chromatogram (TIC) from the Agilent 5973 mass selective detector was used to determine DHO and reference concentrations.

The experimental methods and parameters for observation of DHO/OH reaction products were similar to those for reaction rate experiments, except that the reference compound was excluded from the reaction mixture and the DHO concentration was increased to 1–3 ppm. The reaction mixtures were irradiated for 2–10-s intervals followed by sample collection. Commercially available samples of the identified products were analyzed to verify matching ion spectra and chromatographic retention times.

When possible, the loss of the parent DHO was plotted against the formation of products, generating a straight line with a slope equal to the product yield (Fig. 2). Product quantitation was performed using the Agilent 6890/5973 GC/MS system.

Derivatization of aldehydes and ketones was initiated by flowing of 15–25 L of chamber contents at 3.8 L min^{-1} through 3 mL of acetonitrile in an impinger with no effort to prevent acetonitrile evaporation during sample collection. The sample was removed from the impinger and 200 μL of 0.25-M PFBHA was added to derivatize aldehyde and ketone reaction products to oximes [32] over a 24–48-h time period in the dark. The reacted solutions were gently blown to dryness with UHP N_2, reconstituted with 100 μL of methanol, and 1 μL of the reconstituted solution was injected into the Varian 3800/Saturn 2000 GC/MS system. The derivatization of hydroxy groups (either alcohol or carboxylic acid) was achieved by subsequent addition of 100 μL of commercially available BSTFA to the PFBHA oximes reconstituted with 100 μL of hexane:methylene chloride (1:1). These PFBHA/BSTFA solutions were heated to approximately 60°C for 45 min to complete the silylation, and then 1 μL of the solution was injected into the Varian 3800/Saturn 2000 GC/MS system [32].

All measurements were at least duplicated. A relative standard deviation (the data set standard deviation divided by the data set average) of approximately 2.5% was achieved with the described sampling method utilizing the Entech 7100/Agilent 6890/5973 cryogenic sampling GC/MS system. To determine possible chromatographic interferences from reference/OH reaction products, both DHO and the reference compounds were reacted with the OH radical in separate experiments and analyzed as described above. No chromatographic interferences were observed. Two experiments were conducted to determine the stability of the reference and DHO coexisting in the same bag. First the reference and DHO were injected into the bag, analyzed, photolyzed for 6 min and reanalyzed. Then methyl nitrite, NO, the reference, and DHO were injected into the bag, analyzed, left several hours, and then reanalyzed. None of these preliminary experiments yielded chromatographic peak interferences or observable reactions occurring without photoinitiation. At the end of each run, the Teflon® bag was cleaned by flushing the bag 6 times with ultrapure air (<0.1 ppm total hydrocarbon). Measurements of an air-filled bag showed no cross contamination between runs.

RESULTS

Hydroxyl Radical/DHO Reaction Rate Constant

The OH rate constant for 3,5-dimethyl-1-hexyn-3-ol (DHO, $HC{\equiv}CC(OH)(CH_3)CH_2CH(CH_3)_2$) was obtained using the relative rate method described above. Typically, five experimental runs were conducted on each DHO/reference pair. The plot of a modified version of Eq. (6) is shown in Fig. 1. The $\ln([R]_0/[R]_t)$ term is divided by the respective reference rate constant [decane $(11.0 \pm 2.2) \times 10^{-12}$ cm^3 molecule^{-1} s^{-1} and pentanal $(28.5 \pm 8.6) \times 10^{-12}$ cm^3 molecule^{-1} s^{-1})] [20,37] and multiplied by 10^{-12} cm^3 molecule^{-1} s^{-1} resulting in a unitless number. This yields a slope that is equal to the hydroxyl radical/DHO rate constant, k_{DHO}, *divided by* 10^{-12} cm^3 molecule^{-1} s^{-1}. This modification allows for a direct comparison of the two reference compound/DHO data sets. The slope of the line shown in Fig. 1 yields a hydroxyl radical bimolecular rate constant, k_{DHO}, of $(28.8 \pm 1.2) \times 10^{-12}$ cm^3 molecule^{-1} s^{-1}. The data points at the origin are experimental points because pre-irradiation, $t = 0$, data showed no detectable loss of DHO or reference. The error in the rate constant stated above is the 95% confidence level from the random uncertainty in the slope. Incorporating the uncertainties associated with the reference rate constants (±30% for pentanal and ±20% for decane) used to derive the DHO/OH rate constant yields a final value for k_{DHO} of $(29 \pm 9) \times 10^{-12}$ cm^3 molecule^{-1} s^{-1} [12,13,37].

The DHO/OH rate constant, k_{DHO}, has not been previously reported. The observed rate constant can be compared with a $k_{DHO} = 17 \times 10^{-12}$ cm^3 molecule^{-1} s^{-1}, calculated using a structure reactivity relationship [21]. The calculated value is lower than the measured value reported here and may be due in part to underestimation of OH addition to the carbon–carbon triple bond or OH abstraction of the alkyne hydrogen in DHO.

DHO/OH Reaction Products

The reaction products observed from the initial DHO/OH hydrogen abstraction or OH addition to the triple bond are consistent with previously observed hydroxyl radical reaction mechanisms for oxygenated organic species [14–20]. Typically, the oxygenated organic parent compound reacts with OH to subsequently generate other oxygenated organic products. For DHO, the DHO/OH reaction products observed and positively identified, using the pure compound for verification either by direct gas-phase detection or derivatization or both, were acetone ($(CH_3)_2C{=}O$), 3-butyne-2-one (3B2O, $HC{\equiv}C(=O)(CH_3)$), 2-methylpropanal ($H(O{=})CCH(CH_3)_2$), 4-methyl-2-pentanone (MIBK, $CH_3C(=O)CH_2CH(CH_3)_2$), ethanedial (GLY, $HC(=O)C(=O)H$), and 2,3-butanedione (23BD, $CH_3C(=O)C(=O)CH_3$) and are listed in Table I. Many other DHO/OH reaction products were observed utilizing the derivatization methods described above. Elucidation of these other reaction products was facilitated by mass spectrometry of the derivatized reaction products coupled with plausible DHO/OH reaction mechanisms based on previously published volatile organic compound/OH gas-phase reaction mechanisms [12,14–20,26]. These other reaction products are listed in Table II.

The results for both the positively identified reaction products and the other observed reaction products are described below. The reported yields for MIBK and 3B2O are based on the slopes of the DHO reacted versus product formed plots. The reported error in the product yield is the 95% confidence level from the random uncertainty in the slope of these plots.

Because the DHO/OH reaction products could also react with OH, the observed product concentrations had to be corrected for OH + reaction product reactions.

Table I Molecular Structure and Confirmation Method of Some DHO/OH Reaction Products

DHO/OH Reaction Product Name	Molecular Structure	Confirmation Method(s)
Acetone		Oxime derivatization
4-Methyl-2-pentanone	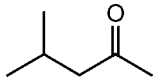	Direct gas-phase detection and oxime derivatization
3-Butyne-2-one	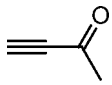	Direct gas-phase detection and oxime derivatization
2-Methylpropanal	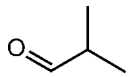	Oxime derivatization
Ethanedial	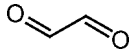	Oxime derivatization
2-Oxopropanal	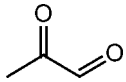	Oxime derivatization
2,3-Butanedione	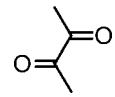	Oxime derivatization

Table II Proposed DHO/OH Reaction Products Based on Data from PFBHA and/or PFBHA/BSTFA Derivatizations

Molecule Name	Molecular Structure
2-Hydroxy-2-methylbut-3-ynal	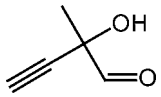
4-Hydroxy-4-methylhex-5-yne-2-one	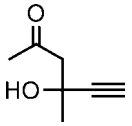
4-Hydroxy-2,4-dimethyl-6-oxohex-5-enal	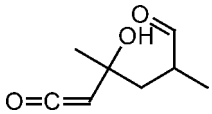
4-Hydroxy-2-methylpentanal	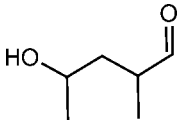
3-Hydroxy-3-methylhex-1-ene-1,5-dione	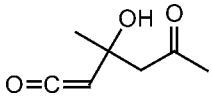

This correction has been described in detail [16,38] and has the following form:

$$F = \frac{(k_{\mathrm{DHO}} - k_{\mathrm{P}})}{k_{\mathrm{DHO}}} \times \frac{1 - \frac{[\mathrm{DHO}]_t}{[\mathrm{DHO}]_0}}{\left(\frac{[\mathrm{DHO}]_t}{[\mathrm{DHO}]_0}\right)^{k_{\mathrm{P}}/k_{\mathrm{DHO}}} - \frac{[\mathrm{DHO}]_t}{[\mathrm{DHO}]_0}} \quad (7)$$

F, the correction factor, was multiplied by the product concentration data; k_{DHO} is the OH + DHO rate constant, and k_{P} is the rate constant for the reaction of OH with reaction product. The measured value for k_{P} was used when possible, but k_{P} was calculated using structure–reactivity relationships [21] when no measured value was available in the literature. It should be noted that the observed reaction products exhibited linear concentration profiles. The lack of curvature strongly suggests that no unusual side reactions generated or removed primary reaction products. For completeness, the k_{P} values are presented with the respective product. The only quantified DHO/OH reaction products were 4-methyl-2-pentanone (MIBK, $CH_3C(=O)CH_2CH(CH_3)_2$) and 3-butyne-2-one (3B2O, $HC{\equiv}CC(=O)CH_3$) because both DHO and these reaction products were the only compounds observed with the cryogenic sampling/Agilent 6890/5973 GC/MS analysis system. The many other products observed utilizing the PFBHA or PFBHA/BSTFA derivative/Varian 3800 Saturn 2000 GC/MS analysis system were not quantified because DHO loss due to reaction with OH could not be determined simultaneously since DHO is not derivatized by PFBHA or PFBHA/BSTFA. Additionally, many of the proposed reaction products are not commercially available, preventing synthesis of oximes to conclusively verify chromatographic and mass spectra data.

Derivatization of nonsymmetric carbonyls using PFBHA or PFBHA/BSTFA typically resulted in multiple chromatographic peaks due to geometric isomers of the oximes. Identification of multiple peaks of the same oxime compound is relatively simple since the mass spectra for each chromatographic peak are almost identical. Typically, the PFBHA derivatized oximes' (generic structure: $F_5C_6CH_2ON{=}C(R_1)(R_2)$) mass spectra included an ion at m/z 181 ($[CH_2C_6F_5]^+$ fragment) with a large relative intensity (>40%) and a [PFBHA oxime + 181]$^+$ ion (due to reactions in the ion trap mass spectrometer) [32]. In most cases the m/z 181 ion relative intensity for the chromatographic peaks due to DHO/OH reaction product oximes was either the largest or one of the largest in the mass spectrum and was used to generate selected ion chromatograms [32]. The mass spectra of compounds that were additionally derivatized with BSTFA had m/z 73 ions from the $[Si(CH_3)_3]^+$ fragments [32]. The product data are described below.

3-Butyne-2-one (3B2O, $HC{\equiv}CC(=O)CH_3$)

3-Butyne-2-one was identified using the Agilent 6890/5973 GC/MS system and quantified using Agilent Chem Station extracted ion analysis of the total ion chromatogram. The 3B2O yield was determined to be $(8.4 \pm 0.3)\%$. Though not previously measured, a value of 9.25×10^{-12} cm^3 molecule^{-1} s^{-1} was calculated for $k_{3\mathrm{B2O}}$ using structure–reactivity relationships and was used in Eq. (7) [21]. From Eq. (7) the average [3B2O] correction was 26% (maximum correction 44%). The PFBHA-3B2O oxime had retention times of 12.2 and 12.6 min, determined utilizing the Varian 3800/Saturn 2000 GC/MS system. Pure 3B2O and synthesis of the 3B2O oxime was utilized to confirm chromatographic results.

4-Methyl-2-pentanone (MIBK, $CH_3C(=O)CH_2CH(CH_3)_2$)

4-Methyl-2-pentanone (methyl isobutyl ketone, MIBK) was identified using the Agilent 6890/5973 GC/MS system and quantified using Agilent Chem Station extracted ion analysis of the total ion chromatogram. The yield data (MIBK/OH corrected) are

plotted in Fig. 2 and resulted in a (26 ± 1.6)% product yield. The rate constant, k_{MIBK}, has been measured [12] and a value of 14.5×10^{-12} cm^3 molecule^{-1} s^{-1} was used in Eq. (7). From Eq. 7 the average [MIBK] correction was 41% (maximum correction 72%). The PFBHA-MIBK oxime had retention times of 14.0 and 14.2 min, determined utilizing the Varian 3800/Saturn 2000 GC/MS system. Pure MIBK and synthesis of the MIBK oxime were utilized to confirm chromatographic results.

The following chronological chromatographic retention time results and mass spectra data were observed utilizing PFBHA or PFBHA/BSTFA derivatization and the Varian 3800/Saturn 2000 GC/MS system. The reaction products reported here had chromatographic peak areas proportional to initial DHO concentration and were observed only after OH initiation of DHO/methyl nitrite/NO/air mixtures. Derivatization experiments performed in the absence of DHO did not result in any of the data reported below except for acetone, which was also observed in pre-photoinitiated DHO/OH derivatization samples. However, the acetone oxime peak area increased with DHO/OH reaction initiation, indicating that acetone is a likely product of the DHO + OH reaction. Aside from the positively identified reaction products (Table I) with the synthesis of the derivatized oxime compound, DHO/OH reaction product identification was derived from mass spectra data and previously published VOC/OH reaction mechanisms [12–20,26].

Acetone ($(CH_3)_2C{=}O$)

The acetone oxime (PFBHA=$C(CH_3)_2$) was observed at approximately 11.2 min employing the Varian 3800/Saturn 2000 GC/ion trap mass spectrometer system described above. Acetone oxime was synthesized to confirm this chromatographic assignment. Acetone oxime was observed in pre-photolysis samples, but the peak area increased upon initiation of DHO/OH reaction indicating acetone as a DHO/OH reaction product.

2-Methyl-propanal (2MP, $HC(=O)CH(CH_3)_2$)

The 2MP oxime (PFBHA=$CHCH(CH_3)_2$) was observed at 12.2 min. 2MP oxime was synthesized to confirm this chromatographic assignment.

Retention Time 14.3 min

The oxime observed with chromatographic peak at retention time of 14.3 min had ions of m/z 42, 55, 112, 181, 292, 293, and a low relative intensity m/z 474 (293 + 181) ion. Using the derivatized molecular weight of 293 for the oxime suggests a ketone with a molecular weight of 98. The single chromatographic peak suggests an aldehyde structure or a symmetric ketone structure. A proposed DHO/OH reaction product assignment of 2-hydroxy-2-methylbut-3-ynal ($H(O{=})CC(OH)(CH_3)C{\equiv}CH$) was made on the basis of the observed data.

Retention Times 15.6 and 16.0 min

One of the largest product peaks observed, the oxime observed with chromatographic peaks at retention times of 15.6 and 16.0 min had ions of m/z 59, 72, 181, 253, 296, and 312. Importantly, the m/z 59 ion had a larger relative intensity than the m/z 181 ion. Using the derivatized molecular weight of 312 for the oxime suggests a ketone with a molecular weight of 117. The PFBHA/BSTFA derivatization method described above yielded a chromatographic peak with a 17.6 min retention time and a mass spectrum with a large relative intensity m/z 131 ion and additional ions of m/z 73, 181, 255, 310, and 368. If the large m/z 59 ion observed in the PFBHA derivatized sample is due to the $[HC(OH)(CH_3)CH_2]^+$ fragment, then additional derivatization by BSTFA on the alcohol group would result in a fragment with m/z 131. Additionally, the PFTBA/BSTFA m/z 368 ion is 72 mu larger than the m/z 296 ion observed in the PFTBA derivatization sample only. A proposed DHO/OH reaction product assignment of 4-hydroxy-2-methylpentanal ($HC(OH)(CH_3)CH_2CH(CH_3)C(=O)H$) was made on the basis of the observed data. The molecular weight of 4-hydroxy-2-methylpentanal is 116, and so the m/z 312 ion observed from PFTBA derivatization could be due to a derivatized molecular weight +1 (M + 1), ion which is a common occurrence in mass spectrometry.

Retention Time 18.1 min

This DHO/OH reaction product was observed after PFBHA/BSTFA derivatizations and had a retention time of 18.1 min. The major ions were m/z 45, 73, 117, 181, 269, 285, 361, 391, and 466. Assuming that the m/z 391 ion is the doubly derivatized (one PFBHA and one BSTFA) reaction product, a molecular weight of 124 can be calculated. The m/z 117 ion could be due to the $[C(=O)OSi(CH_3)_3]^+$ fragment, indicating that this compound could be a carboxylic acid with an additional ketone or aldehyde [32]. Incorporation of the molecular structural elements, the molecular weight, and potential reaction mechanisms did not result in a plausible reaction product molecular structure that would be consistent with all the observed data. Currently, the

identity of this compound is unknown and proposal of a potential reaction product's molecular structure would be pure speculation.

Retention Time 18.8 Through 19.2 min

The oxime observed with chromatographic peaks over the retention time span of 18.8–19.2 min had ions at m/z 43, 98, 123, 140, 181, 252, 279, 320, and 337. Assuming a PFBHA derivatized molecular weight of 337 for the oxime indicates a reaction product molecular weight of 142. There are three distinct chromatographic peaks and one broad peak suggesting an unsymmetrical ketone with multiple derivatization sites. A proposed DHO/OH reaction product assignment of 3-hydroxy-3-methyl-hex-1-ene-1,5-dione ($O{=}C{=}CHC(CH_3)(OH)CH_2C(=O)CH_3$) was made on the basis of the observed data.

Ethanedial (GLY, $HC(=O)C(=O)H$)

The chromatographic peaks for the oxime observed at 20.9 and 21.0 min had ions at m/z 117, 181, 251, 253, 267 (very low relative intensity) and 448 (relative intensity 25% of the m/z 181 ion). The m/z 448 ion is the result of a double PFBHA derivatization indicating a reaction product with a molecular weight of 58. The PFBHA-GLY oxime was synthesized to confirm this chromatographic assignment.

2-Oxopropanal (MGLY, $CH_3C(=O)C(=O)H$)

The single peak for the oxime observed at 21.3 min had ions at m/z 117, 181, 265, 432, and 462. The m/z 462 ion is the result of a double PFBHA derivatization indicating a reaction product with a molecular weight of 72. The PFBHA-MGLY oxime was synthesized to confirm this chromatographic assignment.

2,3-Butanedione (23BD, $CH_3C(=O)C(=O)CH_3$)

The single chromatographic peak for the oxime observed at 21.6 min had ions at m/z 42, 117, 181, 279, 446, 456, and 476. The 476 ion is the result of a double PFBHA derivatization indicating a compound with a molecular weight of 86. The PFBHA-23BD oxime was synthesized to confirm this chromatographic assignment.

Retention Time 23.4 min

The oxime compound at retention time 23.4 min had ions at m/z 181, 295, and low relative intensities for m/z 307 and 311. Assuming the oxime molecular weight is 311 yields a reaction product molecular weight of 116. Interestingly, the addition of the BSTFA derivatization step resulted in a disappearance of this chromatographic peak unlike any other PFBHA-derivatized reaction product. A chromatographic peak at 23.1 min with ions of m/z 73, 181, 255, 265, 367, 383, 549, and 564 was observed after PFBHA/BSTFA derivatization of the reaction products. Adding the mass of $[Si(CH_3)_3]$ in the place of an alcoholic hydrogen to both the m/z 295 ion and the m/z 311 ion could result in corresponding ions of m/z 367 and 383, respectively, observed in the PFBHA/BSTFA derivatized samples. The data suggests that this reaction product contains both a carbonyl group (C═O) and an alcohol group (C─OH), but incorporation of the structural elements, the molecular weight, and potential reaction mechanisms did not result in a plausible reaction product molecular structure that would be consistent with all the observed data. Currently, the identity of this compound is unknown and proposal of a potential reaction product's molecular structure would be pure speculation.

Retention Time 23.8 and 24.0 min

The oxime compound at retention times 23.8 and 24.0 min had ions at m/z 69, 82, 96, 110, 181, 280, 307, and 321. Assuming 321 as the derivatized molecular weight, a reaction product molecular weight of 126 can be derived. A proposed DHO/OH reaction product assignment of 4-hydroxy-4-methyl-hex-5-yne-2-one ($HC{\equiv}CC(OH)(CH_3)CH_2C(=O)CH_3$) was made on the basis of the observed data.

Retention Time 24.1 Through 24.3 min

Chromatographic peaks with some of the largest peak areas were observed for the oxime compound at retention times 24.1 through 24.3 min with ions m/z 43, 57, 83, 251, 295, 333, 351, 491, 531, and 549. Assuming 351 as the derivatized molecular weight yields a reaction product molecular weight of 156. The multiple chromatographic peaks suggest an unsymmetrical ketone with possible multiple derivatization sites. A proposed DHO/OH reaction product assignment of 4-hydroxy-2,4-dimethyl-6-oxo-hex-5-enal ($O{=}C{=}CHC(OH)(CH_3)CH_2CH(CH_3)C(=O)H$) was made on the basis of the observed data.

DISCUSSION

OH reacts with DHO by H atom abstraction or OH addition to the carbon–carbon triple bond [12].

The "reactive structure" of DHO can be drawn as shown in structure 1:

$$\underset{\text{I}\quad\text{II}\qquad\qquad\text{III}\quad\text{IV}\quad\text{V}\quad\text{VI}}{\text{HC}\equiv\text{C}-\text{C(OH)(CH}_3)-\text{CH}_2-\text{CH(CH}_3)_2}$$

1

DHO is a molecule with five distinct sites for possible hydrogen abstraction (I, III, IV, V, VI) and one site for OH addition (II). Site I has a negligible contribution to the DHO/OH rate constant [21], site II contributes approximately 64%, site IV contributes 16%, and site V contributes 14% to the structure reactivity calculated DHO/OH rate constant of 17×10^{-12} cm^3 molecule^{-1} s^{-1} [21]. These three molecular groups contribute approximately 94% to the value of the calculated rate constant. This calculated value is in agreement with the measured value reported here [$(29 \pm 9) \times 10^{-12}$ cm^3 molecule^{-1} s^{-1}), considering that OH rate constants calculated using structure reactivity are typically within a factor of 2 of the measured OH rate constant [21]. A difference between the calculated and measured rate constant could be the group substituent factor of 1.6 used for OH addition to the carbon–carbon triple bond, based on a $-C(OH)H_2$ group and not on $-C(OH)(CH_3)-$ [21]. A larger group substituent factor would increase the calculated DHO/OH rate constant. To date, DHO represents one of the largest alkynes to be investigated for an OH radical reaction rate constant and subsequent gas-phase mechanism. The OH radical combustion and atmospheric mechanisms of the alkyne acetylene (C_2H_2) have received the most research attention. [12,13,24–28].

The experimental parameters were set to minimize other side reactions and highlight the first OH hydrogen abstraction and OH addition step. Nitric oxide (NO) was added to facilitate the generation of OH and to minimize ozone (O_3) and NO_3 formation, preventing other possible radical reactions. The possible mechanistic steps leading to product formation are described below. For some reaction products there may be multiple pathways. Depending on the nature of the radical formed in reaction (4), some of the possible mechanisms for the observed reaction products are as given below.

For acetone (ACE) formation:

$$\text{HC}\equiv\text{CC(OH)(CH}_3)\text{CH}_2\text{CH(CH}_3)_2 + \text{OH} \rightarrow \text{HC}\equiv\text{CC(OH)(CH}_3)\text{CH}_2\text{C}(\bullet)(\text{CH}_3)_2 + \text{H}_2\text{O} \quad (8)$$

$$\text{HC}\equiv\text{CC(OH)(CH}_3)\text{CH}_2\text{C}(\bullet)(\text{CH}_3)_2 + \text{O}_2 \rightarrow \text{HC}\equiv\text{CC(OH)(CH}_3)\text{CH}_2\text{C(OO}\bullet)(\text{CH}_3)_2 \quad (9a)$$

$$\text{HC}\equiv\text{CC(OH)(CH}_3)\text{CH}_2\text{C(OO}\bullet)(\text{CH}_3)_2 + \text{NO} \rightarrow \text{NO}_2 + \text{HC}\equiv\text{CC(OH)(CH}_3)\text{CH}_2\text{C(O}\bullet)(\text{CH}_3)_2 \quad (9b)$$

$$\text{HC}\equiv\text{CC(OH)(CH}_3)\text{CH}_2\text{C(O}\bullet)(\text{CH}_3)_2 \rightarrow \text{beta scission} \rightarrow \underline{\text{O}=\text{C(CH}_3)_2}\text{(ACE)} + \text{HC}\equiv\text{CC(OH)(CH}_3)\text{CH}_2\bullet \quad (9c)$$

For 3-butyne-2-one (3B2O) and 2-methyl propanal (2MP) formation:

$$\text{HC}\equiv\text{CC(OH)(CH}_3)\text{CH}_2\text{CH(CH}_3)_2 + \text{OH} \rightarrow \text{HC}\equiv\text{CC(OH)(CH}_3)\text{C}(\bullet)\text{HCH(CH}_3)_2 + \text{H}_2\text{O} \quad (10)$$

$$\text{HC}\equiv\text{CC(OH)(CH}_3)\text{C}(\bullet)\text{HCH(CH}_3)_2 + \text{O}_2 \rightarrow \text{HC}\equiv\text{CC(OH)(CH}_3)\text{C(OO}\bullet)\text{HCH(CH}_3)_2 \quad (11a)$$

$$\text{HC}\equiv\text{CC(OH)(CH}_3)\text{C(OO}\bullet)\text{HCH(CH}_3)_2 + \text{NO} \rightarrow \text{NO}_2 + \text{HC}\equiv\text{CC(OH)(CH}_3)\text{C(O}\bullet)\text{HCH(CH}_3)_2 \quad (11b)$$

$$\text{HC}\equiv\text{CC(OH)(CH}_3)\text{C(O}\bullet)\text{HCH(CH}_3)_2 \rightarrow \text{beta scission} \rightarrow \text{HC}\equiv\text{CC(OH)(CH}_3)\bullet + \underline{\text{O}=\text{CHCH(CH}_3)_2}\text{ (2MP)} \quad (11c)$$

$$\text{HC}\equiv\text{CC(OH)(CH}_3)\bullet + \text{O}_2 \rightarrow \text{HO}_2 + \underline{\text{HC}\equiv\text{CC}(=\text{O})\text{(CH}_3)}\text{(3B2O)} \quad (11d)$$

For 4-methyl-2-pentanone (MIBK):

$$\text{HC}\equiv\text{CC(OH)(CH}_3)\text{CH}_2\text{CH(CH}_3)_2 + \text{OH} \rightarrow \text{H(HO)C}=\text{C}(\bullet)\text{C(OH)(CH}_3)\text{CH}_2\text{CH(CH}_3)_2 \quad (12)$$

$$\text{H(HO)C}=\text{C}(\bullet)\text{C(OH)(CH}_3)\text{CH}_2\text{CH(CH}_3)_2 + \text{O}_2 \rightarrow \text{H(HO)C}=\text{C(OO}\bullet)\text{C(OH)(CH}_3)\text{CH}_2\text{CH(CH}_3)_2 \quad (13a)$$

$$\text{H(HO)C}=\text{C(OO}\bullet)\text{C(OH)(CH}_3)\text{CH}_2\text{CH(CH}_3)_2 + \text{NO} \rightarrow \text{H(HO)C}=\text{C(O}\bullet)\text{C(OH)(CH}_3)\text{CH}_2\text{CH(CH}_3)_2 + \text{NO}_2 \quad (13b)$$

$$\text{H(HO)C}=\text{C(O}\bullet)\text{C(OH)(CH}_3)\text{CH}_2\text{CH(CH}_3)_2 \rightarrow \text{beta scission} \rightarrow \text{H(HO)C}=\text{C}=\text{O(?)} + \bullet\text{C(OH)(CH}_3)\text{CH}_2\text{CH(CH}_3)_2 \quad (13c)$$

$$\bullet\,\text{C(OH)(CH}_3)\text{CH}_2\text{CH(CH}_3)_2 + \text{O}_2 \rightarrow \underline{\text{C}(=\text{O})\text{(CH}_3)\text{CH}_2\text{CH(CH}_3)_2}\text{ (MIBK)} + \text{HO}_2 \quad (13d)$$

The variety of molecular structures of the DHO/OH reaction products, both identified and proposed, are due to multiple hydrogen abstraction sites on the DHO molecule, the carbon–carbon triple bond on one end of the DHO molecule, and the length of the carbon chain on the other end of the DHO molecule [39].

Most of the previously published alkyne/OH reaction investigations were conducted in the interest of understanding atmospheric and combustion chemistry [12,13,24–28]. Only a few alkyne/OH reactions have been investigated more than once, with acetylene receiving the most attention. The recommended alkyne/OH rate constants for acetylene, propyne, and 2-butyne at atmospheric pressure and ~298 K are 9×10^{-13}, 5.9×10^{-12}, and 27.4×10^{-12} cm^3 molecule^{-1} s^{-1}, respectively [12,24]. The increase in alkyne/OH rate constant is proportional to alkyne chain length and may be due in part to stabilization of the electronically excited alkyne-OH adduct, which could minimize adduct decomposition to initial reactants [12,26,28]. The DHO/OH rate constant reported here [$(29 \pm 9) \times 10^{-12}$ cm^3 molecule^{-1} s^{-1}] is close in value to the 2-butyne/OH rate constant, which may suggest that there is a stabilization limit.

Previous investigations of the alkyne/OH reaction mechanism have identified the most significant reaction step as the addition of the OH radical into the carbon–carbon triple bond yielding an electronically excited species (for acetylene/OH, it is proposed to be $C_2H_2OH^*$). From previous investigations, the fate of this excited species is dependent on pressure, temperature, alkyne carbon chain length, and oxygen concentration [24–28]. Hatakeyama et al. determined the main reaction products of the acetylene/OH reaction to be HCOOH [formic acid, (40 ± 10)% yield) and HC(═O)C(═O)H (GLY, (70 ± 30)% yield] [26]. The observed DHO/OH reaction products at atmospheric pressure were consistent with previously reported alkyne/OH reaction products, but additional reaction products were observed because of DHO's more unusual molecular structure (Tables I and II) [12,13,24–28].

Recently, PFBHA-coated solid-phase microextraction (SPME) fibers were used for the passive sampling of the gas-phase reaction products of *Z*-3-hexen-1-ol/OH, 2-methyl-3-buten-2-ol/OH, and a series of diols/OH. These reactions yielded products that supported OH addition to carbon–carbon double bond and hydrogen abstraction from the C—H bonds of HC(OH) groups [40,41]. However, OH addition to the DHO carbon–carbon triple bond one of the expected reaction products, 3,5-dimethyl-1-hexyn-1,3-diol ($HOC{\equiv}CC(OH)(CH_3)CH_2CH(CH_3)_2$), was unfortunately not observed in the experimental system described above, because this reaction product is not expected to be derivatized by the PFBHA or PFBHA/BSTFA methods described [32].

The combination of PFBHA/BSTFA derivatizations was used recently to identify the reaction products and propose reaction mechanisms for the ozonolysis of α-pinene and Δ^3-carene [32,33]. The separate use of PFBHA and PFBHA/BSTFA derivatizations was critical for insight into the molecular structure of the DHO/OH reaction products. Comparison of the chromatographic and mass spectroscopic results from the PFBHA and PFBHA/BSTFA methods highlighted the portions of the DHO/OH reaction product molecules that contained alcohol or carboxylic acid groups such as was observed for the proposed reaction product 4-hydroxy-2-methylpentanal ($HC(OH)(CH_3)CH_2CH(CH_3)(C(=O)H)$).

CONCLUSIONS

The OH radical can either abstract hydrogen or add to the carbon–carbon triple bond of DHO. A bimolecular rate constant, k_{DHO}, of $(29 \pm 9) \times 10^{-12}$ cm^3 molecule^{-1} s^{-1} was measured using the relative rate technique.

The identification and quantitation of the DHO/OH reaction products was facilitated by the use of derivatizing agents PFBHA and BSTFA. While many DHO/OH reaction products were simply proposed the basis of observed experimental data and previously published VOC/OH reaction mechanisms, several reaction products such as acetone, 4-methyl-2-pentanone (MIBK), 3-butyne-2-one (3B2O), 2-methyl-pentanal ethanedial, 2-oxopropanal, and 2,3-butanedione were positively identified. The structures of the identified reaction products indicate that the carbon–carbon triple bond and the hydrocarbon side chain play important roles in the formation of DHO/OH reaction products through radical stabilization, methyl group transfer, and/or hydrogen-transfer isomerization.

The author wishes to thank the reviewers for their thorough assessment of the manuscript prior to publication.

BIBLIOGRAPHY

1. Mendell, M. J.; Fisk, W. J.; Kreiss, K.; Levin, H.; Alexander, D.; Cain, W. S.; Girman, J. R.; Hines, C. J.; Jensen, P. J.; Milton , D. K.; Rexroat, L. P.; Wallingford, K. M. Am J Pub Health 2002, 92, 1430–1439.
2. Delfino, R. J. Env Health Perspect 2002, 110 supp 4, 573–589.

3. Wilkins, C. K.; Clausen, P. A.; Wolkoff, P.; Larsen, T. S.; Hammer, M.; Larsen, K.; Hansen, V.; Nielsen, G. D. Env Health Perspect 2001, 109, 937–941.
4. Wolkoff, P.; Clausen, P. A.; Wilkins, C. K.; Nielsen, G. D. Indoor Air 2000, 10, 82–91.
5. Wolkoff, P.; Clausen, P. A.; Wilkins, C. K.; Hougaard K. S.; Nielsen, G. D. Atmos Environ 1999, 33, 693–698.
6. Rohr, A. C.; Wilkins, C. K.; Clausen, P. A.; Hammer, M.; Nielsen, G. D.; Wolkoff, P.; Spengler, J. D. Inhala Tox 2002, 14, 663–684.
7. Bodin, A.; Linnerborg, M.; Nilsson, J. L.; Karlberg, A. T. Chem Res Toxicol 2003, 16, 575–582.
8. Nielsen, G. D. Crit Rev Toxicol 1991, 21, 183–208.
9. Kreiss, K.; Gomaa, A.; Kullman, G.; Fedan, K.; Simoes, E. J.; Enright, P. L. N Engl J Med 2002, 347, 330–338.
10. Weschler, C. J. Sci World 2001, 1, 443–457.
11. Weschler, C. J.; Shields, H. C. Atmos Environ 1997, 31, 3487–3495.
12. Atkinson, R. J Phys Chem Ref Data, Monograph 1, 1989.
13. Atkinson, R. J Phys Chem Ref Data, Monograph 2, 1994.
14. Wells, J. R.; Wiseman, F. L.; Williams, D. C.; Baxley, J. S.; Smith, D. H. Int J Chem Kinet 1996, 28, 475–480.
15. Smith, D. F.; McIver, C. D.; Kleindienst, T. E. Int J Chem Kinet 1995, 27, 453–472.
16. Smith, D. F.; Kleindienst, T. E.; Hudgens, E. E.; McIver, C. D.; Bufalini, J. J. Int J Chem Kinet 1992, 24, 199–215.
17. Wallington, T. J.; Andino, J. M.; Potts, A. R.; Rudy, S. J.; Siegl, W. O.; Zhang, Z.; Kurylo, M. J.; Huie, R. E. Environ Sci Technol 1993, 27, 98–104.
18. Veilerot, M.; Foster, P.; Guillermo, R.; Galloo, J. C. Int J Chem Kinet 1996, 28, 235–243.
19. Wyatt, S. E.; Baxley, J. S.; Wells, J. R. Int J Chem Kinet 1999, 31, 551–557.
20. Bradley, W. R.; Wells, J. R.; Wyatt, S. E.; Henley, M. V.; Graziano, G. M. Int J Chem Kinet 2001, 33, 108–117.
21. Handbook of Property Estimation Methods for Chemicals: Environmental and Health Sciences; Boethling, R. S.; Mackay, D. (Eds.); Lewis Publishers: New York, 2000; pp. 335–354.
22. Organic Indoor Air Pollutants: Occurrence, Measurement, Evaluation; Salthammer, T. (Ed.); Wiley-VCH: New York, 1999.
23. Salthammer, T.; Schwartz, A.; Fuhrmann, F. Atmos Environ 1999, 33, 75–84.
24. Sørensen, M.; Kaiser, E. W.; Hurley, H. D.; Wallington, T. J.; Nielsen, O. J. Int J Chem Kinet 2003, 35, 191–197.
25. Atkinson, R.; Aschmann, S. M. Int J Chem Kinet 1984, 16, 259–268.
26. Hatakeyama, S.; Washida, N.; Akimoto, H. J Phys Chem 1986, 90, 173–178.
27. Siese, M.; Zetzsch, C. Zeit fur Physik Chemie 1995, 188, 75–89.
28. Bohn, B.; Siese, M.; Zetzsch, C. J Chem Soc Faraday Trans 1996, 92(9), 1459–1466.
29. Atkinson, R.; Carter, W. P. L.; Winer, J. N.; Pitts, Jr., J. N. J Air Pollut Control 1981, 31, 1090–1092.
30. O'rji, L. N.; Stone, D. A. Int J Chem Kinet 1992, 24, 703–710.
31. Williams, D. C.; O'rji, L. N.; Stone, D. A. Int J Chem Kinet 1993, 25, 539–548.
32. Yu, J.; Flagan, R. C.; Seinfeld, J. H. Env Sci Technol 1998, 32, 2357–2370.
33. Fick, J.; Pommer, L.; Nilsson, C.; Andersson, B. Atmos Environ 2003, 37, 4087–4096.
34. Weschler, C. J.; Shields, H. C. Env Sci Technol 1997, 31, 3719–3722.
35. Weschler, C. J.; Shields, H. C. Environ Sci Technol 1996, 30, 3250–3258.
36. Sarwar, G.; Corsi, R.; Kimura, Y.; Allen, D.; Weschler, C. J. Atmos Environ 2002, 36, 3973–3988.
37. Taylor, W. D.; Allston, D.; Moscato, M. J. Fazekas, G. D.; Kozlowski, R.; Takacs, G. A. Int J Chem Kinet 1980, 12, 231–240.
38. Atkinson, R. Atmos Chem Phys Discuss 2003, 3, 4183–4358.
39. Bethel, H. L.; Atkinson, R.; Arey, J. Environ Sci Technol 2001, 35, 4477–4480.
40. Reisen, F.; Aschmann, S. M.; Atkinson, R.; Arey, J. Environ Sci Technol 2003, 37, 4664–4671.
41. Bethel, H. L.; Atkinson, R.: Arey, J. J Phys Chem A 2003, 107, 6200–6205.